

Muscle Activity Distribution Features extracted from HD sEMG to perform Forearm pattern Recognition

F. Nougarou, A. Campeau-Lecours, Md. R. Islam, D. Massicotte and B. Gosselin

Abstract— An efficient pattern recognition system based exclusively on forearm surface Electromyographic (sEMG) signals is proposed to provide a more intuitive control of a robotic arm used by some of the disabled. The main contribution of this paper is the use of an original set of features characterizing the muscle activity distribution obtained with high-density sEMG (HD sEMG) sensors. Contrary to simple sEMG, HD sEMG can produce muscle activity images with spatial distributions that differ according to forearm movement. In order to translate this distribution, the proposed set of features includes the center of gravity, the mean amplitude and the percentage of influence computed in each HD sEMG image divided in sub-images. Based on these features, the recognition system locates nine forearm movements with high classification accuracies (99.23%). The results in terms of the number of learning data, the image resolutions (spatial filtering) and the number of sub-images demonstrate the potential of the proposed recognition system and its good performance-complexity trade-off.

I. INTRODUCTION

Used on a daily basis by some disabled, JACO [1]-[2], from Kinova Robotics and illustrated in Fig. 1, is a 6 degree of freedom robotic arm with 3 flexible fingers mounted on a wheelchair and controlled by a sensitive Joystick. However, an alternative control has to be developed for disabled people who have limited forearm movement [1]. In order to provide such a control, an accurate pattern recognition system is proposed in this paper, exclusively based on sEMG signals without the help of an inertial measurement unit (IMU) as in [2], pointless for the targeted persons.

Based on two main steps (features extraction and classification), the general goals of pattern recognition are to accurately recognize a maximum number of patterns in real-time execution while being robust in terms of the electrode displacements [3]-[5]. Many studies in literature have focused on the use of single sEMG electrodes and have provided efficient sets of features [6]-[7] and many methods of classification [7]. However, the strategy, with single sEMG, appears unsuitable for real world usage; being too sensitive to electrodes positioning and displacements [4]-[5].

Research supported by ReSMIQ (CANADA).

F. Nougarou is with the Dept. of Electrical and Comp. Engineering, University of Québec at Trois-Rivières and Laval University, Québec, CANADA (e-mail: francois.nougarou@uqtr.ca)

A. Campeau-Lecours is with the Dept. of Mechanical Engineering, Laval University, Québec, CANADA (e-mail: Alexandre.Campeau-Lecours@gmc.ulaval.ca)

Md. R. Islam and D. Massicotte are with the Dept. of Electrical and Comp. Engineering, University of Québec at Trois-Rivières, Québec, CANADA (e-mail: Md.Rabiul.Islam@uqtr.ca & daniel.massicotte@uqtr.ca)

B. Gosselin is with the Dept. of Electrical and Comp. Engineering, Laval University, Québec, CANADA (e-mail: benoit.gosselin@gel.ulaval.ca)

The use of HD sEMG can fix this issue. The application of spatial filtering can reduce the drift effect [8]-[9] and the overall information from HD sEMG can appear unchanged for some displacements [5].

This study exploits the large surface of two HD sEMG sensors to perform a forearm pattern recognition of high accuracy with a reasonable complexity with the potential to control JACO in real-time, Fig. 1. To do this, an original set of features characterising the muscle activity distribution extracted from HD sEMG sensors is proposed and applied to a classifier based on the linear discriminant analysis (LDA) [7]. At each 100ms, a HD sEMG sensor produces an image of muscle activity from which three different resolutions are obtained applying spatial filtering [8]. Each obtained image is divided into sub-images of equal size in which three features are computed: the coordinates of the center of gravity, the mean amplitude and the percentage of influence. These features take advantage of the HD sEMG sensors to characterize the spatial distribution of muscle activity obtained from different movements. As used and mentioned in [10], the center of gravity has been employed extensively in fundamental research with HD sEMG to determine and analyze changes in muscle activity recruitment strategies.

This paper is organized as follows: Section II describes the proposed set of features for the pattern recognition; the experimentation and the results obtained as concerns the amount of data used during the learning phase of the LDA, the number of sub-images used in the method and the combination of image resolutions appear in Section III; some discussion ensues about the performance-complexity trade-offs that the proposed set of features offers; finally, Section IV draws some brief conclusions.

II. PATTERN RECOGNITION SYSTEM DESCRIPTION

The proposed system of pattern recognition is depicted in Fig. 1. Details on each part of the system appear below.

A. Data acquisition & filtering

Two HD sEMG sensors placed on the forearm can be seen as $N_r \times N_c$ matrices of sEMG electrodes. The electrode at row i and column j records the signal $e_{i,j}[n]$, the voltage between its position and the ground (the monopolar mode); with $i = 1, 2, \dots, N_r$, $j = 1, 2, \dots, N_c$ and $n = 1, 2, \dots, N$ where N is the number of samples with a sampling frequency of $F_s = 2048$ Hz. All $e_{i,j}[n]$ signals were applied to a 30 to 450 Hz band-pass 4th order Butterworth and to notch filters at 60 Hz and its harmonics to remove ECG and the power line interferences.

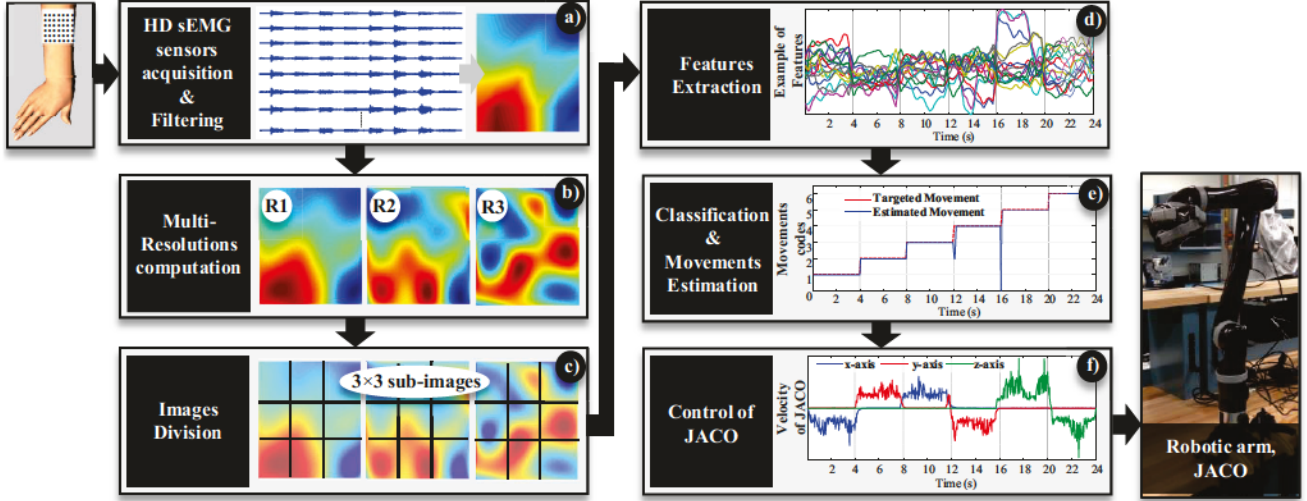


Fig. 1. Proposed pattern recognition system with its main steps and illustrations of a) obtained RMS image of muscle activity from one HD sEMG sensor at a given moment, b) obtained resolutions (R1, R2 and R3) after spatial filtering, c) images division for 3×3 sub-images, d) an example of muscle activity distribution features (center of gravity coordinates), e) targeted movements codes (red) and estimated movements codes after the classification for 6 movements, and f) an example of velocities of JACO according to axes obtained during its real-time control. In this example, the movements codes 1 to 6 respectively control negative displacements on the x-axis, positive displacements on the y-axis, positive displacements on the x-axis, negative displacements on the y-axis, positive displacements on the z-axis and negative displacements on the z-axis.

B. Multi-resolution computation

As previously explained, the structure of a HD sEMG sensor can return some images of the forearm muscle activity at different moments, see Fig. 1.a. In order to extract more information from HD sEMG, in addition to monopolar mode information (1), two different spatial filters are computed at each sample n : bipolar filter (2) and inverse binominal (3) filter [8]. These three types of image resolutions correspond to different spatial selectivities which represent the muscle activity at different depths [9].

$$e_{i,j}^{R1}[n] = e_{i,j}[n] \quad (1)$$

$$e_{i,j}^{R2}[n] = e_{i,j}[n] - e_{i-1,j}[n] \quad (2)$$

$$\begin{aligned} e_{i,j}^{R3}[n] = & 12e_{i,j}[n] - e_{i-1,j+1}[n] - e_{i+1,j-1}[n] - e_{i+1,j+1}[n] \dots \\ & - e_{i-1,j-1}[n] - 2e_{i+1,j}[n] - 2e_{i,j+1}[n] - 2e_{i-1,j}[n] - 2e_{i,j-1}[n] \end{aligned} \quad (3)$$

C. Images division & features extraction

The extraction of features is based on the amplitude of signals expressed by the root mean square (RMS) value applied to non-overlapping windows of 100ms, which are compliant with real-time usage. Indeed, the recognition process has to be performed in 300ms to remain undetectable to users [6]. The RMS value for the window w from the signal $e_{i,j}^{R1}[n]$ of row i and column j is defined in (4), where $w = 1, 2, \dots, N_w$ is the index of the N_w windows. $N_w = \lceil N / N_s \rceil$ with $\lceil \cdot \rceil$ the round down operation and $N_s = \lceil 0.1 \times F_s \rceil$ the number of samples in a 100ms window, indexed by $v = 1, 2, \dots, N_s$. The RMS is computed for the two other resolutions to obtain their amplitude representation $a_{i,j}^{R2}[w]$ and $a_{i,j}^{R3}[w]$. Fig. 1.b. presents an example of RMS images for all resolutions at a given w .

$$a_{i,j}^{R1}[w] = \sqrt{\frac{1}{N_s} \sum_{v=1}^{N_s} e_{i,j}^{R1}[(w-1)N_s + v]^2} \quad (4)$$

The first step of the proposed features extraction consists in dividing each RMS image w in N_d sub-images of equal size. $N_d = \sqrt{N_d}$ is an integer defining the number of divisions applied to the row and the column. An illustration of a division of images into $N_d = 3 \times 3$ sub-images is shown in Fig. 1.c. Considering the same number of rows and columns in HD sEMG, $N_r = N_c$, the number of rows and columns per sub-images is defined by $U = \lceil N_r / N_d \rceil = \lceil N_c / N_d \rceil$. The indexes of divisions per row and column are respectively $\varepsilon_r = 1, 2, \dots, N_d$ and $\varepsilon_c = 1, 2, \dots, N_d$. The indexes of the rows and columns per sub-images are $u_r = 1, 2, \dots, U$ and $u_c = 1, 2, \dots, U$. The sub-images are $N_d \times N_d$ matrices indexed with ε_r and ε_c .

The three proposed features of the sub-image for the row ε_r and the column ε_c applied to $a_{i,j}^{R1}[w]$ at each w are the following:

- The coordinates of the Center of Gravity (CG) [10], $x_{\varepsilon_r, \varepsilon_c}^{R1}[w]$ (5) and $y_{\varepsilon_r, \varepsilon_c}^{R1}[w]$ (6), characterize the orientation of muscle activity [10] of a given sub-image. $\mathbf{p} = [1, 2, \dots, N_r]$ and $\mathbf{z} = [1, 2, \dots, N_c]$ are the required vectors of values of the rows and the columns. An example of the CG coordinates is presented in Fig. 1.d.

$$x_{\varepsilon_r, \varepsilon_c}^{R1}[w] = \frac{\sum_{u_r=1}^U \sum_{u_c=1}^U \chi[(\varepsilon_r - 1)U + u_r] a_{(\varepsilon_r - 1)U + u_r, (\varepsilon_c - 1)U + u_c}^{R1}[w]}{\sum_{u_r=1}^U \sum_{u_c=1}^U a_{(\varepsilon_r - 1)U + u_r, (\varepsilon_c - 1)U + u_c}^{R1}[w]} \quad (5)$$

$$y_{\varepsilon_r, \varepsilon_c}^{R1}[w] = \frac{\sum_{u_r=1}^U \sum_{u_c=1}^U p[(\varepsilon_r-1)U+u_r] a_{(\varepsilon_r-1)U+u_r, (\varepsilon_c-1)U+u_c}^{R1}[w]}{\sum_{u_r=1}^U \sum_{u_c=1}^U a_{(\varepsilon_r-1)U+u_r, (\varepsilon_c-1)U+u_c}^{R1}[w]} \quad (6)$$

- The mean amplitude, $\alpha_{\varepsilon_r, \varepsilon_c}^{R1}[w]$ is computed in all sub-images using (7). This feature discriminates the movements in function of amplitude and localisation (position of the sub-image) over all moments w .

$$\alpha_{\varepsilon_r, \varepsilon_c}^{R1}[w] = \frac{\sum_{u_r=1}^U \sum_{u_c=1}^U a_{(\varepsilon_r-1)U+u_r, (\varepsilon_c-1)U+u_c}^{R1}[w]}{U \times U} \quad (7)$$

- The percentage of influence, $\beta_{\varepsilon_r, \varepsilon_c}^{R1}[w]$, computed in all sub-images as (8), represents an additional information on the amplitude distribution of all images w .

$$\beta_{\varepsilon_r, \varepsilon_c}^{R1}[w] = \alpha_{\varepsilon_r, \varepsilon_c}^{R1}[w] / \left(\frac{1}{N_\rho \times N_\chi} \sum_{\rho=1}^{N_\rho} \sum_{\chi=1}^{N_\chi} \alpha_{\rho, \chi}^{R1}[w] \right) \quad (8)$$

These three features are computed for all resolutions and HD sEMG sensors. The total size of the proposed set is $N_{gf} = N_f \times N_\varepsilon \times N_{res} \times N_{mat}$ for each w , with N_f the number of features for a given image, N_{res} the number of resolutions and N_{mat} the number of the used HD sensors.

D. Classification










The goal of this paper is to observe the impact of the proposed features with a typical classifier. In literature, the LDA appears the most popular techniques for pattern recognition based on EMG [7]. During its learning phase, the LDA computes coefficients from its inputs and knowledges of the movements. During the estimation phase, these coefficients estimate a movement code $\hat{m}[w]$ (Fig. 1.e) at each w based on the features of unknown patterns. The LDA complexity directly depends on the number of inputs, N_{gf} .

III. EXPERIMENTATION DESCRIPTION AND RESULTS

A. Experimentation and cross-validation

Two 8×8 HD sEMG sensors (64-channels sEMG, ELSCH064NM3, OT Bioelettronica; Torino, Italy) were placed on the posterior and anterior sides of the right forearm of a healthy subject near the elbow. The nine movements including the rest, described in Table I, were performed during each of the 20 recorded trials. For all trials, all movements were separated from the others by an

TABLE I. PERFORMED HAND AND WRIST MOVEMENTS

1. Rest		4. Ulnar flexion		7. Extension	
2. Fist		5. Radial flexion		8. Pronation	
3. Spread		6. Flexion		9. Supination	

interval of 5s of rest and were successively performed in the same order and held for 5s.

The cross-validation scheme was used to accurately evaluate the simulated pattern recognition systems [4]. All recorded data was separated into two sets: learning and evaluation data. The learning data is expressed in terms of trials which represent 5s of data for each movement. Based on the 20 trials, the 19 possibilities of cross-validation were considered in order to observe the impact of the number of trials to compute the LDA: from the use of 1 trial to find the movements of the other 19 trials, to the use of 19 trials to find the movements of 1 trial.

The pattern recognition systems are evaluated in terms of mean error (in %) obtained from the evaluation data. These results correspond to the mean of 500 combinations of a given cross-validation possibility (except for the validations with less combinations) of the mean error from all nine patterns. Moreover, a set of features composed of the RMS values for each electrode $a_{i,j}^{R1}[w]$, $a_{i,j}^{R2}[w]$ and $a_{i,j}^{R3}[w]$ for the two HD sEMG sensors is used as reference, as used in [5]. Since the proposed features are constructed from the RMS values, a comparison with this reference permits observing the improvement obtained with the proposed set.

B. Pattern recognition Results

Fig. 2 shows the recognition results of the proposed set of features for different divisions and different sizes of learning data, and permits making the following observations:

- First, considering the case of the 19 trials to compute the LDA coefficients, the pattern recognition system achieves a mean error inferior to 1% using the proposed features with 3×3 and 4×4 sub-images and inferior to 2% with 2×2 sub-images.
- Moreover, the three configurations (2×2, 3×3, and 4×4 sub-images) produce better results than the RMS features regardless of the number of learning trials.
- The interest of the images division is evident when comparing with the results of the method without

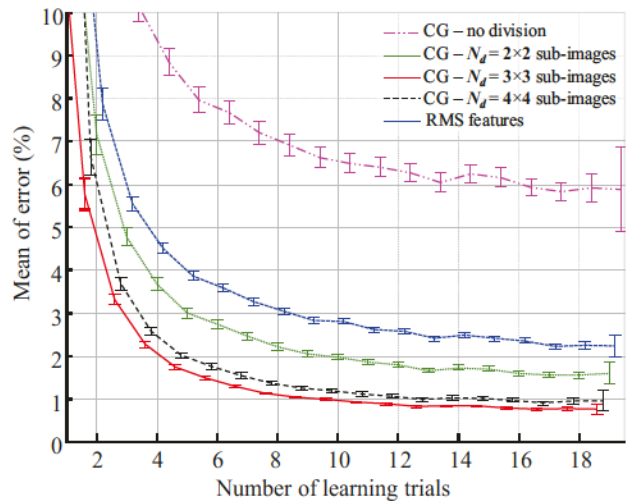


Fig. 2. Mean error for pattern recognition systems based on the proposed set of features referred as CG with 0, 2×2, 3×3 and 4×4 sub-images and based on the RMS features, for 2 HD sEMG sensors and the 3 resolutions in function of the trials number used to compute the LDA coefficients.

TABLE II. NUMBER OF THE FEATURES IN FUNCTION OF THE MATRICES AND IMAGES CONFIGURATIONS

Matrices and images configurations	Type of feature			
	CG - 2×2	CG - 3×3	CG - 4×4	RMS
2 matrices / R1	32	72	128	72
2 matrices / R2	32	72	128	72
2 matrices / R3	32	72	128	72
2 matrices / R1+R2	64	144	256	144
2 matrices / R1+R3	64	144	256	144
2 matrices / R2+R3	64	144	256	144
2 matrices / R1+R2+R3	96	216	384	216

division, higher than 5% error rate. With 3×3 sub-images, the results are better than with 2×2. And for 4×4 sub-images, a performance loss is noted due to the RMS values reduction.

- The system of pattern recognition with the features from 3×3 sub-images presents the best performances. With 4 learning trials, this set of features achieves the same performance as the RMS features with 19 learning trials (close to 2 % error rate). With 8 learning trials, the proposed features with 3×3 sub-images obtains an error rate close to 1%, while the RMS features produces 3% error. As presented in Table II, these two sets of features have the same number of values: in both cases, the LDA classifier presents the same complexity. The use of 2×2 sub-images represents a good performance-complexity trade-off: it achieves better performances than the RMS features with only 96 inputs (instead of 216 inputs).

In Fig. 3, considering the proposed set of features with 3×3 sub-images and 2 HD sEMG sensors, every combination of the computed resolutions is compared.

- Based only on the monopolar and the inverse binomial resolutions, the features extracted method with 3×3 sub-images returns higher errors than the reference method.
- However, with the bipolar resolution, the proposed features return the same performance as the reference which uses information from all resolutions. In this case, the proposed set of features permits greatly reducing the number of LDA inputs and the classifier complexity.

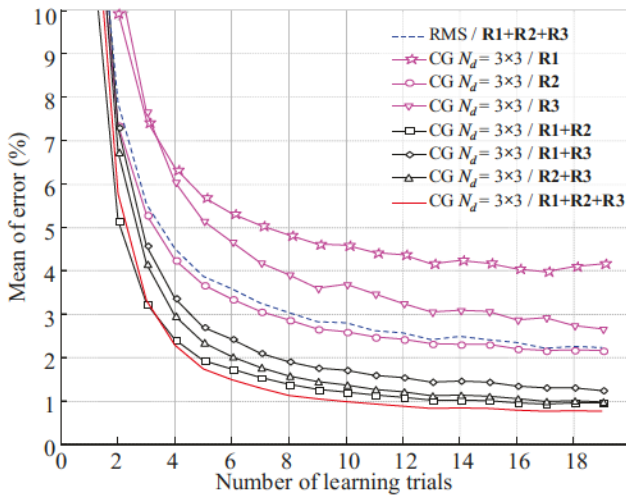


Fig. 3. Obtained mean error for pattern recognition systems based on the proposed set of features with 3×3 sub-images and based on the RMS features, for 2 HD-sEMG sensors and for different combination of resolutions, in function of the trials number used to compute LDA coefficients.

Indeed, as presented in Table II, the set of features obtained with the bipolar resolution (R1) and 3×3 sub-images represents 72 inputs and the RMS features, with all resolutions, 216 inputs: 67% reduction.

- The combination of two resolutions improves the pattern recognition performance, up to 99% accuracy. And the combination of the three resolutions obtains the best performances. However, because the results are close, the two resolutions is a better trade-off of performance-complexity: 144 inputs compared to 216 in Table II.

IV. CONCLUSION

In this paper, an original set of features characterising the muscle activity distribution extracted from HD sEMG sensors is proposed to perform a forearm pattern recognition of high accuracy with a reasonable complexity. Indeed, the proposed set of features takes advantage of the use of HD sEMG sensors which represent a powerful solution allowing the creation of images of the muscle activity at different resolutions. In addition, each image is divided into sub-images to improve the features extraction. The simulations have shown that the proposed set used allows reaching high performance (up to 99% accuracy) while respecting realistic learning conditions. These features can also provide a good performance-complexity trade-off. Future studies will continue and analyze the real-time performance of the proposed method to control the robotic arm JACO and analyze its performance with more efficient classifiers.

REFERENCES

- [1] CL Fall, G Gagnon-Turcotte, JF Dube, JS Gagne and Y Delisle, A Campeau-Lecours, C Gosselin, B Gosselin, "A Wireless sEMG-Based Body-Machine Interface for Assistive Technology Devices," *IEEE Journal of Biomedical and Health Informatics*, IEEE Journal of Biomedical and Health Informatics, vol. 21, no. 4, pp. 967-977, 2017.
- [2] U. Côté-Allard, F. Nougrou, C. L. Fall, P. Giguere, C. Gosselin, F. Laviolette et B. Gosselin, "A convolutional neural network for robotic arm guidance using sEMG based frequency-features", *IEEE/RSJ Int. Conf. on Intelligent Robots and Systems*, Octobre 2016.
- [3] M. Oskoei and H. Hu, "Myoelectric Control Systems - A survey," *Biomedical Signal Processing and control*, vol. 2, pp. 275-94, 2007.
- [4] J. M. Hahne, B. Graimann and K.R. Muller, "Spatial filtering for robust myoelectric control," *IEEE Trans. Biomed. Eng.*, vol. 59, No. 5, pp. 1436-43, May 2012.
- [5] A. Boschmann and M. Platzner, "Towards robust HD EMG pattern recognition: Reducing electrode displacement effect using structural similarity," *IEEE EMBS conf.*, pp. 4547-50, 2014.
- [6] K. Englehart, B. Hudgins, "A robust, real-time control scheme for multifunction myoelectric control," *IEEE Trans. Biomed. Eng.*, vol. 50, No. 7, pp. 848-54, June 2003.
- [7] L. J. Hargrove, K. Englehart and B. Hudgins, "A Comparison of Surface and Intramuscular Myoelectric Signal Classification," *IEEE Trans. Biomed. Eng.*, vol. 54, No. 5, pp. 847-53, May 2007.
- [8] D. Farina, L. Arendt-Nielsen, R. Merletti, B. Indino and T. Graven-Nielsen, "Selectivity of Spatial Filters for Surface EMG Detection from the Tibialis Anterior Muscle," *IEEE Trans. Biomed. Eng.*, vol. 50, No. 3, pp. 354-64, March 2003.
- [9] D. F. Stegeman, B. U. Kleine, B. G. Lapatki, J. P. Van Dijk, "High-density Surface EMG: Techniques and Application at Motor Unit Level," *Journal of Biocyber. and Biomed. Eng.*, vol. 32, No. 3, pp. 3-27, July 2012.
- [10] J. Abboud, F. Nougrou, M. Loranger, and M. Descarreaux, "Test-retest reliability of trunk motor variability measured by large-array surface electromyography," *Journal of Manipulative Physiol. Ther.*, vol. 38, No. 6, pp. 359-64, July 2015.